

MAS 316: An introduction to chaotic dynamics

160175125

1 Introduction

The following report looks at various different maps and flows which model systems and explores their properties. The goal is to find and explain the different types of solutions that the maps have, how changing the parameters of the maps change the solutions, and what the physical implications of the solutions that we find are. Transitions between stable and chaotic solutions will be of particular interest, with the aim to learn more about when the solutions transition to a chaotic state from a stable state.

2 Bifurcations of 1-d maps

2.1 Lemming population map

Suppose that a population of lemmings is modelled by the map

$$x_{t+1} = rx_t/(1 + x_t^2), \quad x, r \in [0, \infty), \quad (1)$$

where x represents the size of the lemming population, $f(x) = rx/(1 + x^2)$ is the evolution rule of the population, and r is related to the growth rate of the population. We are first asked to find all the fixed points of the system. The fixed points are found precisely when $x_{t+1} = x_t$; let such points be denoted by x_c and substitute this into (1) to get

$$x_c = rx_c/(1 + x_c^2) \Rightarrow x_c^2 + 1 = r,$$

and so

$$x_c = (r - 1)^{1/2}. \quad (2)$$

Then (2) gives all the fixed points of the system as a function of r . We are only interested in populations that are greater than zero, but for $r \leq 1$, (2) shows that x_c is either zero or complex, therefore we take $r > 1$. Now we want to assess the stability of the fixed points to understand the conditions where the lemming population is stable and where it is not. We do this by examining when $|f'(x_c)| < 1$ is satisfied; when the inequality is satisfied the corresponding fixed point is stable, i.e. attracting.

Now

$$f'(x) = \frac{d}{dx} \left(\frac{rx}{1 + x^2} \right) = \frac{2rx^2 - r(1 + x^2)}{(1 + x^2)^2} = \frac{r(x^2 - 1)}{(1 + x^2)^2}, \quad (3)$$

then substituting (2) into the result of (3) yields $f'(x_c) = (r - 2)/r$. Then using ** we have

$$|f'(x_c)| = \frac{|r - 2|}{|r|} < 1. \quad (4)$$

Rearranging (4) gives $r - 2 < r$ (since we take $r > 1$) which holds for all $r > 1$. Therefore any lemming population greater than zero will converge to a stable population size greater than zero, and chaotic lemmings populations can not exist. **Figure 1** shows the lemming population size as time passes for three different values of r , i.e $r \in \{1.1, 20, 50\}$. As r is increased, the lemming population takes longer to reach its equilibrium state and the equilibrium population size also increases.

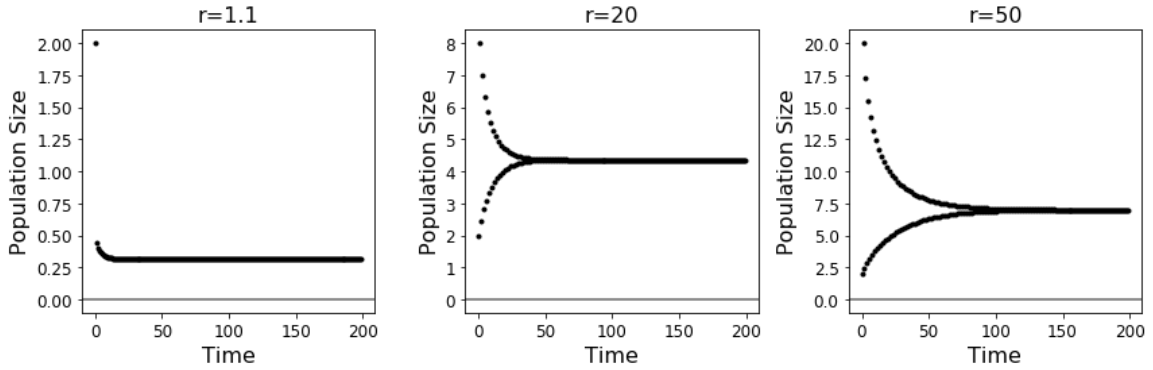


Figure 1: Shows three plots of time series for the lemming population for different values of r . As r is increased the lemming population takes longer to settle down to its stable population size, and the larger r is the larger the stable population size is.

2.2 Electrical current maps

We are now given the following two maps

$$x_{t+1} = e^{-rx_t}, \quad x_{t+1} = r \cos(x_t), \quad (5)$$

which model electrical currents in an electronic component. We can not algebraically manipulate these maps to find where $x_{t+1} = x_t$ so we must find another way to explore them. We can assess the behaviour of the maps and whether they become chaotic through the use of bifurcation diagrams. **Figure 2** shows bifurcation diagrams for each of the maps. Plot **2.(i)** shows a period doubling of the exponential map for $r \gtrapprox 2.6$ where the singular equilibrium becomes unstable and splits into two stable equilibria, so if the decay of the current is large enough, then the current will begin to oscillate within the component. We know that the evolution rule of the exponential map is a solution to a type of linear ODE, so the map can not exhibit chaotic dynamics as non-linearity is necessary for chaos. An example of an electronic component that may exhibit such behaviour is an electronic oscillator, which converts DC current to AC (**Wikipedia.A 2019**). Plot **2.(ii)** shows a bifurcation diagram for the cosine map. We see that increasing the amplitude, r , of the wave causes the electrical current to first begin to oscillate in the component before becoming unstable and chaotic once r is increased further, but also notice the current can return to a stable periodic state if we continue to increase r even further. An example of an electronic component which contains a chaotic electrical

current may contain what is known as a Chua's circuit, or a non-periodic oscillator to give it another name, which produces an oscillating waveform which never repeats (**Wikipedia.B 2019**).

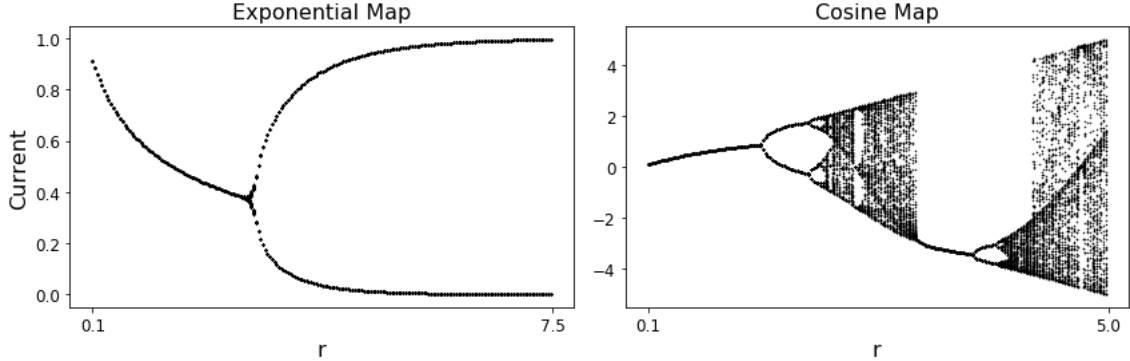


Figure 2: Shows two bifurcation diagrams for the two maps given in (5) respectively. Plot 2.(i) shows a period doubling for the exponential map for sufficiently large r , however due to its linear nature the map can not exhibit chaos. Plot 2.(ii) shows that chaos can occur for the cosine map. Note that it is possible for the map to return to stability as r is further increased.

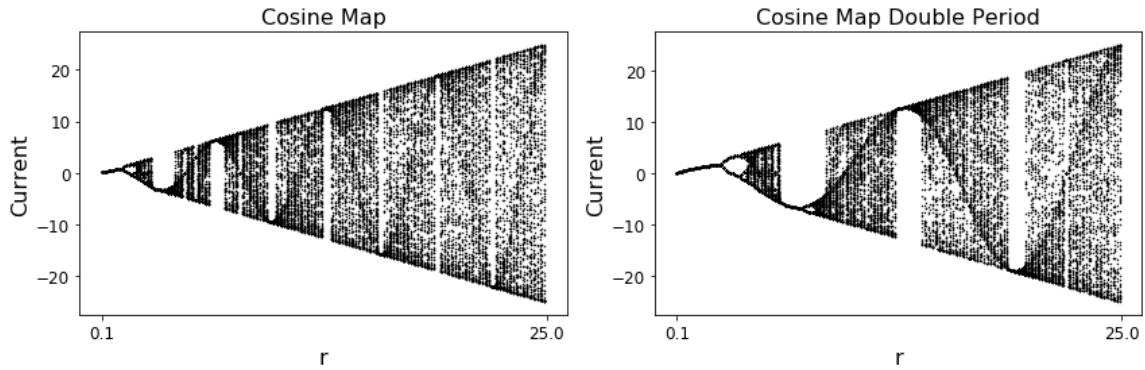


Figure 3: Shows two bifurcation diagrams for the cosine map. Plot 3.(i) is the same diagram as seen in Figure 2.(ii) except more r values have been plotted. Note that the transitions between stability and chaos appear to be predictable and related to the period of the map. Plot 3.(ii) shows the map where the period has been doubled, i.e $x_{t+1} = r \cos(x_t/2)$; we see that the intervals where stability occurs has also doubled which shows that the transition between chaotic and stable behaviour is predictable.

Can we learn any more about the chaotic behaviour we see in the cosine map? **Figure 3** shows more bifurcation diagrams for the cosine map. Plot 3.(i) shows the same diagram as in Figure 2 except larger r values have also been plotted. Plot 3.(ii) shows cosine map where the period has been doubled, i.e $x_{t+1} = r \cos(x_t/2)$. If we first examine plot 3.(i), notice that despite the chaotic behaviour there are some interesting predictable features in the chaos. First note that we see a faint sine wave appearing in the diagram (can be seen more clearly in plot 3.(ii)); we also see that the chaos transitions to stability regularly at the peaks and troughs of the sine wave; we also see that

the wavelength of the map is independent of the amplitude, which implies an increase in the speed at which x changes. Because r only controls the amplitude of the wave, we get a linear squashing in the horizontal direction and stretching in the vertical direction. The interval of stability between the chaos also gets squashed in the same way which enables us to predict which r values give rise to chaos and which do not (not explicitly calculated here). The right plot illustrates the relationship between the period of the map and the r values for which the map is stable further showing the predictability of the chaos in the map.

3 The Tinkerbell map

In this section we examine The Tinkerbell map. The evolution rule for the map is defined as

$$\mathbf{f}(x, y) = (x^2 - y^2 + c_1x + c_2y, 2xy + c_3x + c_4y). \quad (6)$$

We are told to examine a time series of the map using the parameters $\mathbf{c} = (-0.3, -0.6, 2, 0.5)$. **Figure 4** shows a Poincare section of the Tinkerbell map. Each plot shows a different presentation of the Poincare section to enable us to see how the trajectory intercepts the plane. Plot **4.(i)** shows the map where the first 1000 points have not been plotted in order to remove any transient behaviour that exists as it is not what we are interested in. Plot **4.(iii)** shows a zoomed in view of a section of the loop seen in plot **4.(i)**. Both plots appear to show us that the trajectory never intersects the plane where it has intersected previously, and plot **4.(ii)** shows that the map traces out a loop every 30 time steps. Since the trajectory appears to map to a new point every time it intercepts the plane, we have a chaotic attractor.

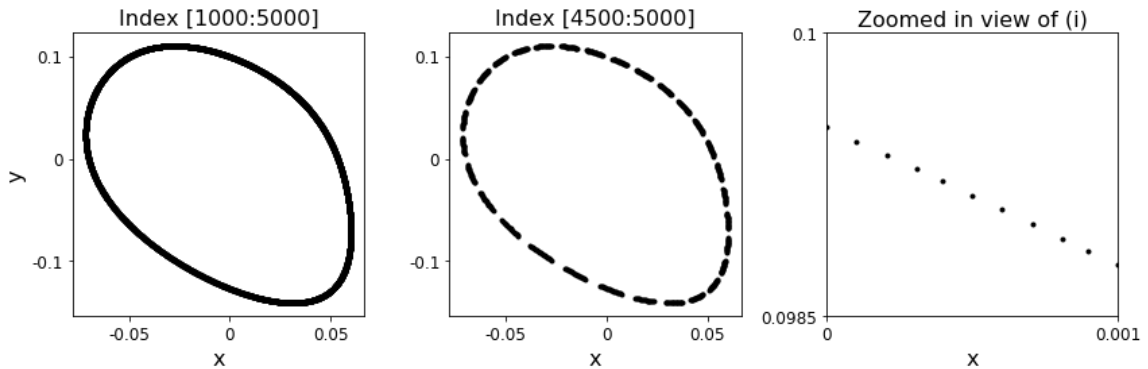


Figure 4: Shows three views of a Poincare section of the Tinkerbell map for the parameters $\mathbf{c} = (-0.3, -0.6, 2, 0.5)$. Plot **4.(i)** shows the map where the first 1000 time points have not been plotted, plot **4.(ii)** shows the map where the first 4500 points have not been plotted, and plot **4.(iii)** shows a zoomed in view of part of the loop in plot **4.(i)**. We see from plot **4.(ii)** that the trajectory traces out a loop every 30 time steps. Plots **4.(i)** & **4.(iii)** show that the trajectory never appears to map onto a point it has previously mapped onto previously, suggesting that the Tinkerbell map is a chaotic attractor.

Next we look at the Tinkerbell map for different choices of c_4 . When c_4 is reduced, the Poincare section looks very similar to the loop in plot **4.(i)** of **Figure 4**, however it loses its shape somewhat

(see **Figure 5**). There is not much else to say about the case for small c_4 . **Figure 6** shows three plots for $c_4 \in \{0.72, 1, 1\}$ respectively. Plot **6.(i)** shows the case where c_4 is increased from 0.6 to 0.72; the increase causes the loop that the trajectory traces out on the plane to become unstable and produces a stable spiral pattern which is converging towards the centre of the loop and looks like a rotating and shrinking pentagon. The centre plot shows the case for $c_4 = 1$, this is very similar to the first case except the increase in c_4 causes the spiral to converge towards the centre more rapidly, so c_4 is acting as a damping term on the attractor. This faster convergence allows us to see the shrinking and rotating pentagon shape more clearly. The right plot also shows the case $c_4 = 1$, this time however only the last 500 time points have been plotted which gives the effect of zooming in on the centre of the spiral in the centre plot. We see that the plots are indistinguishable if not for the labelled scale, which tells us that the trajectory does not converge to an equilibrium, but rather appears to produce an infinite fractal structure. This tells us that the Tinkerbell map has a strange attractor.

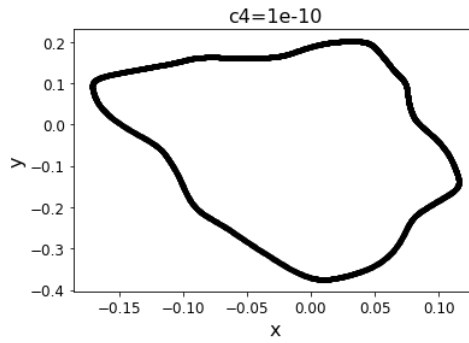


Figure 5: Shows a Poincaré section of the Tinkerbell map when $c_4 = 10^{-11}$. We see that a small value of c_4 has the effect of deforming the loop seen in **Figure 4.(i)**.

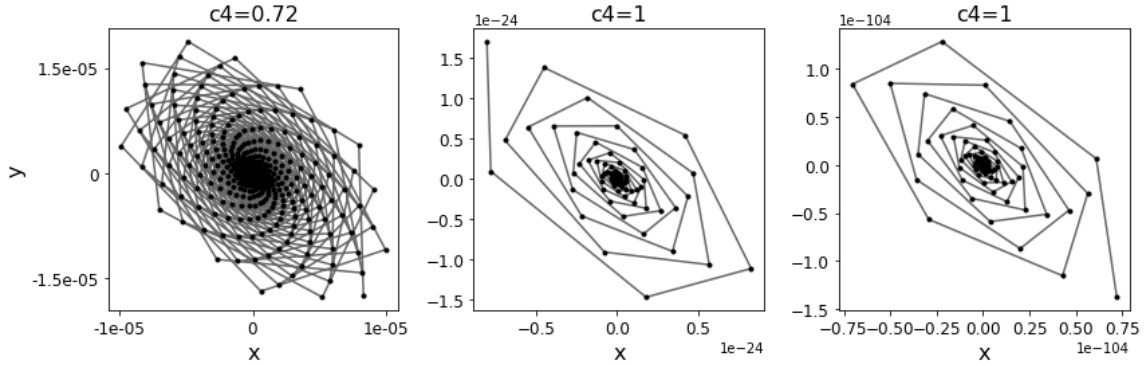


Figure 6: Shows Poincaré sections for the cases $c_4 \in \{0.72, 1, 1\}$ respectively. as c_4 increases, the loop becomes unstable and converges towards the centre of the loop and converges more rapidly the larger r is. Plot **6.(iii)** is a magnified picture of the central region in plot **6.(ii)** and shows evidence that the map does not converge to a singular point, but rather exhibits fractal properties instead.

We now look at another case, given by the parameters $\mathbf{c} = (0.9, 0.6013, 2, 0.5)$, which gives rise to

self-similarity (i.e a fractal structure), by way of plots. **Figure 7** shows a grid of plots for the attractor produced by the given parameters. We see that it appears no matter how far we zoom into the structure, we just see more and more of the same indistinguishable structure where each line seems to have infinitely more lines traced on top of it. This is caused by repeated stretching and folding of the map onto itself for each time step.

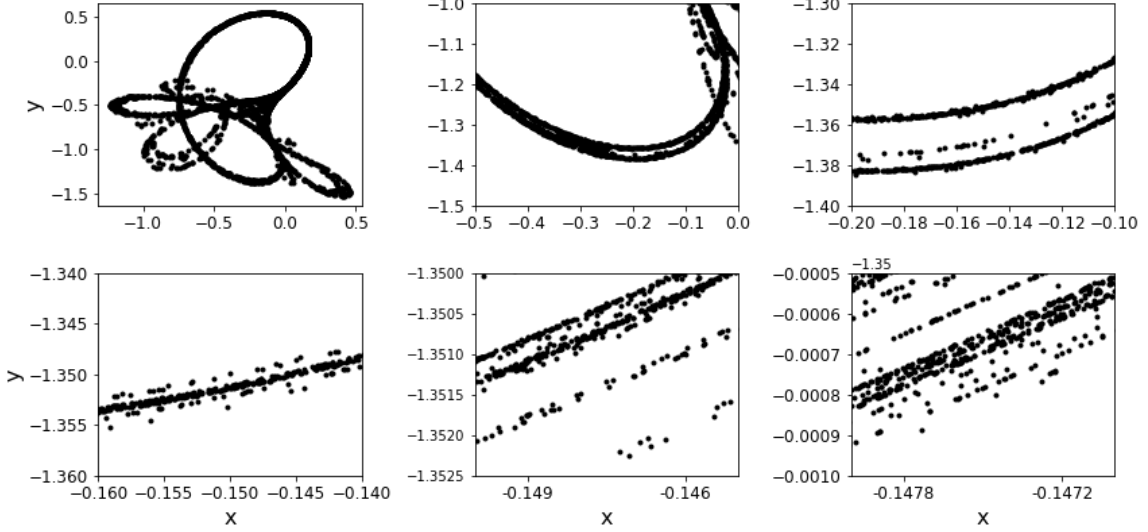


Figure 7: Shows numerous plots of the Tinkerbell map attractor for parameters $\mathbf{c} = (0.9, -0.6013, 2, 0.5)$. Each plot is a successive magnification of a section in the previous plot. We see that no matter how far we zoom into the structure we see more of the same structure, so the plots are essentially indistinguishable in terms of scale.

Also useful to know is the factor by which the Tinkerbell map expands or contracts as a function of x and y . We do this by working out the Jacobian of the system. So the Jacobian is

$$\left| \frac{\partial(x_{t+1}, y_{t+1})}{\partial(x_t, y_t)} \right| = \left| \begin{matrix} 2x_t + c_1 & -(2y_t - c_2) \\ 2y_t + c_3 & 2x_t + c_4 \end{matrix} \right| = (2x_t + c_1)(2x_t + c_4) + (2y_t + c_3)(2y_t - c_2), \quad (7)$$

which gives

$$= 4x_t^2 + 2x_t(c_1 + c_4) + c_1c_4 + 4y_t^2 + 2y_t(c_3 - c_2) - c_2c_3. \quad (8)$$

Now the map will expand whenever the Jacobian is greater than 1, and contract whenever the Jacobian is less than 1. If we examine the terms of (8) we see that the Jacobian is greater than 1 whenever

$$c_2c_3 + 2c_2y_t < 4x_t^2 + 2x_t(c_1 + c_4) + c_1c_4 + 4y_t^2 + 2c_3y_t \quad (9)$$

is satisfied, so the map will expand.

4 A model of sheared fluid flow

In this final section we will look at model which models a sheared fluid flow. The model we will look at is the 2-d Trefethen model, and is defined as

$$\dot{\mathbf{u}} = A\mathbf{u} + \|\mathbf{u}\|B\mathbf{u}, \quad A = \begin{bmatrix} -1/R & 1 \\ 0 & -2/R \end{bmatrix}, \quad B = \begin{bmatrix} 0 & -1 \\ 1 & 0 \end{bmatrix}, \quad (10)$$

where $\mathbf{u} = (u_1, u_2)$ and $\|\mathbf{u}\| = \sqrt{u_1^2 + u_2^2}$, $R > 0$. We are told that the system has an attracting fixed point at $\mathbf{u} = \mathbf{0}$ which represents laminar flow, and we are also told that the system also has a non-zero attracting fixed point which represents turbulent flow. Therefore there is an as yet unknown boundary where laminar flow will transition into turbulent flow; this boundary is what we would like to investigate. Linearisation about the solution $\mathbf{u} = \mathbf{0}$ gives $\dot{\mathbf{u}} = A\mathbf{u}$ which means that whenever $\|\mathbf{u}\| = 0$ we have a laminar flow. The idea then is to perturb the system and look at the value of $\|\mathbf{u}\|$ in the long term, after the transient period, and see whether the value of $\|\mathbf{u}\|$ has returned to zero or not. If $\|\mathbf{u}\| = 0$ after the transient period, then the perturbation was small enough that the flow can return to a laminar state. On the other hand if $\|\mathbf{u}\| > 0$ after the transient period, then the perturbation was too large for the flow to return to a laminar state and the flow is perpetually turbulent.

The natural question to ask then is can we find the maximum perturbation to the flow that still allows the flow to return to a laminar state? We can look for this by plotting $\|\mathbf{u}\|$ against time. **Figure 8** shows three plots for various perturbation sizes of the system $u_2 \in \{10^{-6}, 10^{-5}, 10^{-2}\}$, $R = 25$. We see that for $u_2 \in \{10^{-6}, 10^{-5}\}$ the value of $\|\mathbf{u}\|$ returns to zero after a period of time meaning that the flow is able to return to a laminar state. However for $u_2 = 10^{-2}$ the value of $\|\mathbf{u}\|$ converges to 1, meaning the system was perturbed too much and can not return to a laminar state.

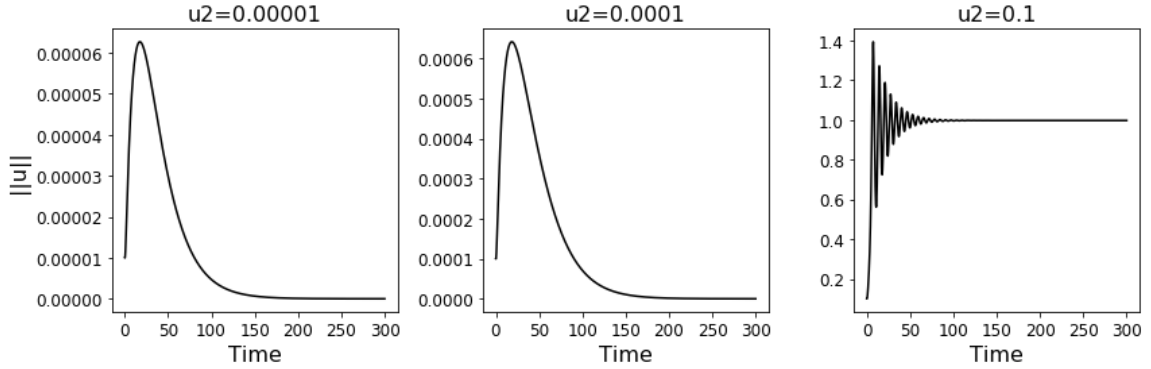


Figure 8: Shows three plots which show the time evolution in the value of $\|\mathbf{u}\|$ for different sized perturbations from the laminar state. Plot **8.(i)** is the case $u_2 = 10^{-6}$; the perturbation is not large enough to cause a permanent transition to the turbulent state. Plot **8.(ii)** is the case $u_2 = 10^{-5}$; again we see that the perturbation is not large enough to cause a permanent transition to the turbulent state. Plot **8.(iii)** is the case $u_2 = 10^{-2}$; we see now that the perturbation is large enough to cause a permanent transition to the turbulent state.

The next figure pinpoints more accurately where the perturbation size increase causes the transition from laminar to turbulent flow. **Figure 9** shows the post transient (equilibrium) value of $\|\mathbf{u}\|$

plotted for various different initial perturbations to the system. We see the point $u_2 \approx 0.00042$ where further increase in the size of the perturbation causes the flow to fail to return to the laminar state $\|\mathbf{u}\| = 0$ for the case $R = 25$.

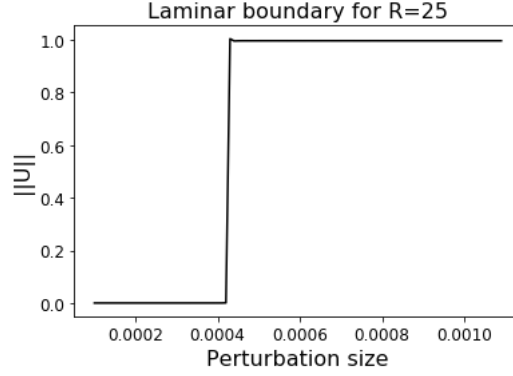


Figure 9: Shows the post-transient value of $\|\mathbf{u}\|$ for various different perturbation sizes. We see that when $u_2 \approx 0.00042$, there is a switch where the perturbation is large enough to cause a permanent transition to the turbulent state.

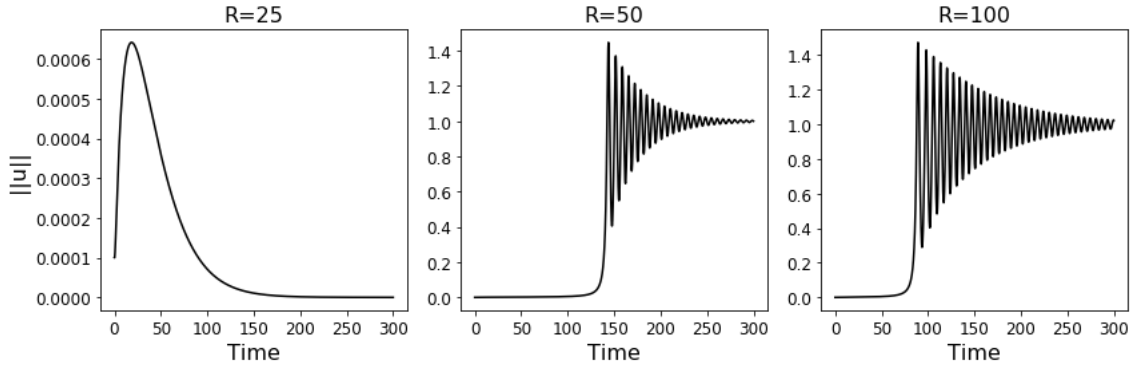


Figure 10: Shows three plots for the same sized perturbation $u_2 = 0.0001$, but different values of R , i.e $R \in \{25, 50, 100\}$ respectively. Plot **10.(i)** is identical to **Figure 8.(i)** where $R = 25$ and is simply for reference. Plot **10.(ii)** shows the case where $R = 50$; we see that the increase in flow rate is enough to cause a permanent transition to the turbulent state. Plot **10.(iii)** is the case $R = 100$; we see that increasing the flow rate further reduces the time taken for the transition to occur and increases the time taken for the flow to converge to the turbulent equilibrium.

The next question we want to know is "How does varying the flow rate R affect the transition to turbulence?". **Figure 10** shows three plots for $R \in \{25, 50, 100\}$ where the perturbation size is $u_2 = 0.0001$. We see that increasing the flow rate also causes perpetually turbulent flows that would have otherwise returned to laminar flow. Also, the higher the flow rate the quicker the flow will transition to the turbulent state and the longer the turbulent state takes to reach its stable equilibrium state. Why is this the case? Well, increasing R means that the linear term $A\mathbf{u}$ in our model (10) becomes smaller relative to the non-linear term $\|\mathbf{u}\|B\mathbf{u}$. When $\|\mathbf{u}\|$ is small, the

non-linear term is also small and does not affect \dot{u} much, but since increasing R reduces the size of the linear term, this is the same as increasing the effect of the non-linear term, which causes the non-linear term to dominate faster. If the perturbation is too small however, the non-linear term stays small so never becomes dominant, and that allows the flow to return to a laminar state. The transition to turbulence is then governed by the ability of the non-linear term to become dominant, and if it can then the flow transitions into a turbulent state.

5 Conclusion

We have seen a number of different solution types arise to various different models. In §2 we saw that solutions experience trans-critical bifurcations during parameter changes where their fixed points suddenly become unstable and the solution has to find another fixed point to converge to. If the solution can not find a stable fixed point then the solution becomes chaotic and never settles down (this is the period doubling route to chaos). In order to get this type of solution however we need non-linearity within evolution rule of the map. In §3 we looked at a two-dimensional non-linear map and found that the solution does not converge, but rather gives rise to fractal structure where the solution essentially becomes independent of scale as it is indistinguishable from itself on both large and small scales, i.e the solution is a strange attractor. Lastly we looked at a two-dimensional model that models sheared fluid flow. We were especially interested in the boundary between when a laminar flow transitions to turbulent flow. We saw that both increasing the initial perturbation, or increasing the flow rate, resulted in a quicker transition from laminar flow to turbulent flow, and saw that this was directly related to whether the non-linear term kills itself off, or whether it grows and dominates the linear terms in the model.

6 Acknowledgements

Thank you to Dr Ashley Willis, and also Dr Sam Dolan, of The University of Sheffield for the material needed to produce this report.

7 References

(Wikipedia.A 2019). *Electronic Oscillator*. https://en.wikipedia.org/wiki/Electronic_oscillator (Accessed online May 2019).

(Wikipedia.B 2019). *Chua's Circuit*. https://en.wikipedia.org/wiki/Chua%27s_circuit (Accessed online May 2019).